Predator-scale spatial analysis of intra-patch prey distribution reveals the energetic drivers of rorqual whale super-group formation

David E. Cade, S. Mduduzi Seakamela, Ken P. Findlay, Julie Fukunaga, Shirel R. Kahane-Rapport, Joseph D. Warren, John Calambokidis, James A. Fahlbusch, Ari S. Friedlaender, Elliott L. Hazen, Deon Kotze, Steven McCue, Michael Meÿer, William K. Oestreich, Machiel G. Oudejans, Christopher Wilke, Jeremy A. Goldbogen

Supporting Information

This combined pdf file contains the following linked sections:

Appendix S1- Detailed methods

Field methods

Operations in South Africa were based on the RV FRS Ellen Khuzwayo and two small boats were launched to conduct tagging and observation work (additional details in Findlay *et al.* 2017). Monterey Bay operations were based on shore with daily excursions in the RV John Martin and two rigid hull inflatable boats (RHIBs); surveys were conducted along the shelf break until blue whales were found. Unlike in South Africa, super-groups were not targeted specifically but were encountered opportunistically and boats often conducted UAV (unoccupied aerial vehicles) and tagging operations around individual whales that were encountered. In both locations whales were approached in a 6 m RHIB and a 6 m pole was used to deploy suction cup attached video and 3D accelerometer tags manufactured by Customized Animal Tracking Solutions (CATS) (Cade *et al.* 2016). When super-groups were found or whales were tagged, the larger RV either conducted additional support operations (e.g. UAV work around tagged animals) or conducted acoustic surveys in a box pattern around tagged whales. All data used in this project were collected under NMFS permits 16111, 14809, and 20430 and South African permits RES2015/DEA and RES2016/DEA.

Foraging behavior

Our analysis of behavior in super-groups consisted of 3D movement data from six tagged humpback whales and six tagged blue whales (Table S2). We deployed two CATS tags on humpback whales in super-group in 2015 as well as four additional tags on whales not in super-groups. One of these animals travelled south for the duration of the deployment (3.5 hrs) and did not feed so was excluded from analysis. In general, periods of super-group activity for humpback whales were directly observed from the surface (mean deployment duration: 6.2 ± 3.9 hrs), however one of the non-super-group animals demonstrated localized, intensive feeding behavior at night and was observed in the morning in the vicinity of > 20 other whales, so this localized feeding bout was included in the super-group analysis. Additional

periods of super-group behavior in 2016 were also identified when direct tag video confirmation could be made of at least six animals feeding within an estimated five body lengths of the tagged whale (Fig 2). In 2016 we deployed six tags on super-group whales, though two were of short duration (<10 minutes) and one collected video but no data; these three were excluded.

We deployed four tags on blue whale in the two described super-groups, and also had two whales with tags on join the super-group on 16 Aug. With much longer deployments averaging 9.5 ± 10.8 hrs during which whales were not observed for the duration of their deployments, periods of blue whale super-group behavior were identified as periods during which the whales were within a restricted region (~ 1 nm across) at the head of the canyon in which the super-group was observed.

Feeding rate analysis

Tag accelerometers for all whales were sampled at 40 or 400 Hz, magnetometers and gyroscopes at 40 or 50 Hz, and pressure, light, temperature and GPS at 10 Hz. All data were decimated to 10 Hz, tag orientation on the animal was corrected for, and animal orientation was calculated using custom-written scripts in Matlab 2014a (following Johnson & Tyack 2003; Cade *et al.* 2016). Animal speed for all deployments was determined using the amplitude of tag vibrations (Cade *et al.* 2018).

Rorqual whale feeding behavior is a constant optimization problem balancing resource acquisition at depth with oxygen acquisition at the surface (Hazen, Friedlaender & Goldbogen 2015). Stereotypical behavior consists of diving from the surface, lunge feeding one to ten times at depths ranging from the surface to > 300 m, then surfacing for one to a dozen or more breaths and then diving to forage again. When this behavior repeats without a prolonged break it is known as a foraging bout. Lunge feeding on krill is highly stereotypical (Goldbogen *et al.* 2006; Cade *et al.* 2016) and individual lunges can be identified from the tag records as peaks in speed followed by rapid deceleration that corresponds to increases in dynamic body acceleration as well as changes in pitch, roll and heading associated with maneuvering (Simon, Johnson & Madsen 2012; Cade *et al.* 2016). Dives to > 5 m were identified as feeding dives if they included at least one lunge. To determine the average duration of foraging bouts across these two species we analyzed

the largest published collection of cetacean bio-logging data from Goldbogen *et al.* (2019), which consisted of 112 feeding blue whales – 67 from Southern California (Cade *et al.* 2016; Southall *et al.* 2019) and 45 from Monterey Bay – and 42 krill-feeding humpback whales – 17 from the West Antarctic Peninsula, 9 from South Africa, 12 from Monterey Bay and 4 from WA inland waters. Foraging bouts were differentiated by examining the distributions of surface intervals between the end of a feeding dive and the start of the next dive (feeding or not). Surface interval for all whales demonstrated clear bi or multimodal distributions (Fig S4), so Gaussian curves were fit (using the fitgmdist function in Matlab 2014a, see Cade & Benoit-Bird 2014) and the first set of curves that best matched the shape of the distribution was selected. AIC and BIC continued to drop as the model complexity increased, but the change was < 5% each time and additional μs were outside the bulk of the data. The surface interval equivalent to the final μ in the bulk of the data plus 3σ was chosen as the value to separate feeding behavior into foraging bouts. Feeding dives separated by more than this inter-bout interval (5.5 minutes for both species) were considered to be part of separate foraging bouts. Feeding rates (lunges/hr within foraging bouts during super-group and non-super-group times) were determined for all whales by dividing the number of lunges by the total duration of all foraging bouts.

Other parameters analyzed, including inter-lunge interval (ILI), dive duration, lunges per dive and search area per lunge were determined on a dive-by-dive scale and averaged. Results in Table S2 are the mean and standard deviation (*SD*) for each super-group whale. ILI is the time (s) between the peak in speed (nearly equivalent to mouth opening time, Cade *et al.* 2016) from one lunge to the next peak in speed in the next lunge of that dive. Dive duration was the time from leaving the surface to reaching the surface for all dives > 5 m (calculated via finddives.m from animaltags.org). Search area between lunges was determined using the geo-referenced pseudotrack (Wilson *et al.* 2007) of the whale, calculated from whale speed, pitch and heading, and then distributing the resulting positional error between every two known positions. The set of spatial x and y coordinates (z was calculated but not used) of the whale between lunges was then used to find the two points that were furthest apart horizontally (p_1 and p_2). Additionally, the points furthest from the line segment $\overline{p_1 p_2}$ (one point above and one below) were identified and the distance from each

point to $\overline{p_1 p_2}$ was calculated. Search area between each pair of lunges in a dive was then calculated as the length of $\overline{p_1 p_2}$ multiplied by the sum of the distances of the two additional points from the line.

Prey data collection

Acoustic backscatter data were collected only during daylight hours using Simrad EK60 or EK80 transceivers with split-beam 38 kHz and either 120 or 200 kHz transducers in both ecosystems. In South Africa, all three frequencies (EK60) were hull mounted on the RV Khuzwayo and transmitted pulses when in the vicinity of whales, but the 120 kHz transducer was only operable for 5 of the 15 sea days. All three transducers had a 7° beam width and operated with a pulse length of 1024 µs. In Monterey Bay, data were collected from two platforms: the RV Martin with all three frequencies hull mounted and pinging continuously and the RHIB Musculus with 38 and 120 kHz transducers pole mounted, running on Ek80 CW mode, and deployed opportunistically when the vessel was available and in the vicinity of tagged whales. On both Monterey Bay vessels, the 38 kHz transducer had a beam width of 12° and used a 1024 µs pulse length and other transducers had 7° beam width with a 512 µs pulse length. Bottom depth in all South Africa humpback whale habitat was < 150 m, above the time-varied gain noise threshold for the 200 kHz transducer at -80 dB. All units reported in dB are S_v (mean volume backscatter strength) re 1 m^2/m^3, except when specifically referencing individual target strength (TS), which is reported in dB re 1 m^2, and when S_a is reported in Fig. S2, which is in dB re 1 m^2/m^2 (see MacLennan, Fernandes & Dalen 2002 for details). Because the 120 kHz transducer was not operable for the bulk of analysis days in South Africa and the 200 kHz had sufficient resolution for the depths of interest (no data deeper than 150 m), for consistency across that ecosystem the 120 kHz data from its five functional days was excluded. In contrast, blue whale habitat was deeper (bottom depth often > 400 m, with dives to krill patches up to 250 m deep), so the 120 kHz was used as the primary comparison to 38 kHz data (which also allowed consistency across Monterey Bay vessels). Relative krill sizes in the two ecosystems (see below) also justified the analytical frequencies.

All systems were calibrated using a 38.1 mm tungsten carbide sphere (Demer *et al.* 2015) as close as possible to the time of data collection. In both field sites this was immediately temporally adjacent to the

second field season for each of the large vessels (RV Martin and RV Khuzwayo) and within a week of all data collected on the Musculus. Echosounders were set to ping between 0.5 to 1.5 s (typical values were 1-1.2 s) based on bottom depths. If false bottoms appeared in the monitored echograms, ping intervals were increased.

Humpback whale super-groups observed in South Africa were tightly spaced (>50 whales in a square region <100-200 m on a side (Fig 2)). The limited maneuverability of the 39 m RV Khuzwayo precluded entry directly into these tight formations, so prey mapping around whales consisted of doing box patterns at distances of 100-500 m from the main group. On one occasion on 3 Nov 2016 the group moved within 100 m of the vessel and forward motion was halted. Due to weather conditions and equipment delays, only one tagged humpback whale foraging in a super-group overlapped with prey mapping around super-groups (Fig 2E), so prey and whale analysis are generally from different super-groups. Blue whale super-groups observed in Monterey Bay were more loosely aggregated and could be maneuvered among, so prey data during super-group events are in and among foraging whales, and six tagged whales fed for at least part of their tagged duration within super-groups (Table S2). Due to competing research priorities, the areas surveyed were at times haphazard, so we could not attempt analyses that depended on the horizontal spatial extent of prey layers but instead focused on prey density near super-groups in comparison to prey density near feeding whales that were not in super-groups.

Prey data processing

Hydroacoustic data were imported into Echoview 9 and each field day was analyzed independently. Standard acoustic processing resulted in the removal of data below the sea floor, general background noise (De Robertis & Higginbottom 2007), additional regions of high noise (common when the ship was maneuvering or in rough seas) and signals from other sonar systems (Ryan *et al.* 2015) across all frequencies. The geometry of the high-frequency (HF, 120 or 200 kHz) and 38 kHz data were matched, and the SHAPES algorithm for school detection (Barange 1994; Coetzee 2000) was applied to a HF-38 dB differenced echogram thresholded at 8 dB (see rationale below).

Mean krill lengths in both ecosystems under study were substantially smaller than the mean lengths of *Euphausia superba* on which the majority of euphausiid hydroacoustic literature focuses (techniques summarized in Jarvis *et al.* 2010). While *E. superba* have seasonal mean lengths that range from 30 to 50 mm (Atkinson *et al.* 2009), measured *E. lucens*, the dominant euphausiid in South Africa, during a cruise concurrent to our field efforts were 14 ± 1.4 mm, and adult *E. pacifica* and *Thysanoessa spinifera*, the dominant Euphausiids in Monterey Bay (Croll *et al.* 2009) and in blue whale diets (Croll *et al.* 2005; Nickels, Sala & Ohman 2018) range from 10.2 ± 3.0 to 16.0 ± 2.0 mm and 15.3 ± 0.2 to 23.7 ± 0.4 mm, respectively, with krill in blue whale fecal samples consistently larger than those found in net tows (Croll *et al.* 2005; Nickels, Sala & Ohman 2019). At a nominal sound speed of 1500 m s^{-1} the wavelengths of 38, 120 and 200 kHz signals are 39.5, 12.5 and 7.5 mm respectively, implying that for zooplankton lacking a resonator (like an air-filled swim-bladder), animals smaller than the wavelength of the signal will have strongly reduced signals (Stanton *et al.* 1994; Stanton, Chu & Wiebe 1998) and additionally implying that dB differencing and target strength (TS) models for larger krill like *E. superba* are not appropriate for the smaller krill in this study. Instead, TS of these krill were calculated using an SDWBA scattering model (as in Conti & Demer 2006), but parameterized with inputs (e.g., animal density and sound speed relative to seawater and krill morphology) measured on krill species which are found in the Monterey Bay study site, *T. spinifera* and *E. pacifica,* and also applied to the similarly-sized *E. lucens*. An average TS for each ecosystem was calculated by averaging (in the linear domain) 1000 simulated krill with lengths from normal distributions determined from representative krill sizes. For *E. lucens* we used our measured lengths, and for Monterey Bay data we used the fecal-sample-determined distribution of *T. spinifera* (the most common blue whale prey as per Nickels, Sala & Ohman 2018; Nickels, Sala & Ohman 2019) from Croll et al. (2005) of 19.3 ± 1.5 mm. Using *E. lucens* length-wet weight curves (Pérez Seijas 1987) and averaging male and female values gave 0.026 g/krill, similar to the 0.025 g/krill derived from a cross-species relationship (Mauchline 1967). We applied the smaller value since our mean sizes were larger than the juvenile *E. lucens* data measured by Pérez Seijas. *T. spinifera* wet weight (0.040 g/krill) was also calculated from the Mauchline curve but restricted to Pacific Ocean *Thysanoessa sp.* and *E. pacifica* measurements. TS

calculated from these lengths and our SWDBA model were -93.2 (@120 kHz) and -93.6 dB re 1 m^2 (@200 kHz) for Monterey Bay *T. spinifera* and South Africa *E. lucens* respectively. At these size ranges, HF minus 38 kHz dB differences ranged from 16-18 dB in Monterey Bay and 23-24 dB in South Africa (mean size ± 2 *SD*). Mean biomass density (*B*) in kg/m^3 at any spatial scale could then be estimated via eq. 1 (as described in Simmonds & MacLennan 2008; Jarvis *et al.* 2010) from the measured mean volumetric backscatter at the corresponding spatial scale (S_v), the estimated TS and the estimated individual krill mass (*M*) in g:

$$B = \frac{10^{\mathrm{Sv}/10}}{10^{\mathrm{TS}/10}} \times \frac{M}{1000} \qquad \text{(eq. 1)}$$

At high frequencies (120 and 200 kHz), euphausiid TS are highly susceptible to changes in orientation, with, for instance, orientation changes of five degrees potentially resulting in 200 kHz TS differences up to 20 dB (Demer & Martin 1995; Stanton & Chu 2000; CCAMLR 2005). Additionally, these relatively large dB differences (compared to the differences centered around 9 dB for *E. superba*, Jarvis *et al.* 2010) often spanned to levels below the detection threshold used for 38 kHz analysis. Consequently, for exclusion of likely non-euphausiid backscatter, a lower threshold of 11.4 dB was used for 200 kHz data and 9.5 dB for 120 kHz data so that krill would not be inappropriately excluded (Warren *et al.* 2001). These thresholds are the mean of the low value used for *E. superba* (Jarvis *et al.* 2010) and the HF-38 differences for the largest krill we measured (18.7 dB at 200 kHz, 14.3 dB at 120 kHz for 35 mm *T. spinifera*). These values should allow our results to be comparable to previous studies that used lower thresholds and also confirmed high krill abundances (using net tows) collocated with high acoustic backscatter in Monterey Bay (Schoenherr 1991; Croll *et al.* 2009; MBNMS 2009; Santora, Ralston & Sydeman 2011).

Siphonophores are known contributors to acoustic backscatter and their presence can bias results (Warren *et al.* 2001; McGarry 2014). To minimize this source of error, we linearly subtracted the backscatter at 38 kHz from the HF backscatter; since siphonophores have resonant air pockets they have similar backscatter at HF as at 38 kHz (Stanton, Chu & Wiebe 1998; Warren *et al.* 2001). All S_v reported are this linearly subtracted value, which were 0.2 ± 0.3 dB and 0.1 ± 0.1 dB lower than the HF values in Monterey Bay and South Africa respectively.

Distribution of resources

To confirm that gulp-sized cells, our base analytical unit, were distributed lognormally, histograms of biomass in gulp-sized cells were examined on a day-by-day basis and in total (Fig. S1). Although most statistical tests for normality are not appropriate for large sample sizes – e.g. total gulp-sized patches within an ecosystem – and are sensitive to outliers (Ghasemi & Zahediasl 2012), a Box Cox transformation on krill density in all gulp-sized cells resulted in a parameter of 0, suggesting the appropriateness of log transforming biomass. For each krill patch identified, a signed rank-sum test comparing the median of all of the gulps within a patch to the overall biomass derived from patch S_v revealed that in three quarters of the cases, gulp medians were significantly different than the linearly averaged S_v of the patch (Fig. S1), suggesting that resources the size of what whales actually feed on (the gulp-sized cell) are not represented by the patch arithmetic mean. Given the lognormal distributions of gulps within patches, the variation in patch sizes, and the variation in the number of acoustic samples per patch in our acoustic surveys, the commonly employed approach of linearly averaging all acoustic data within whole patches or large cells into single values would be likely to skew the data to a degree dependent on the size of the patches and the preponderance of any rare but large data that are unlikely to be encountered by a foraging predator (i.e. outliers).

As an additional line of evidence to determine if there would be a difference between analyzing ecosystem data using gulp-sized cells compared to mean patch densities, we looked at the distributions of gulps within krill patches and used a nonparametric rank-sum test to test if the patch S_v were likely to have been sampled from the observed distribution of gulp sizes. The frequency of times when the null hypothesis could be rejected on each day is shown in Fig S1 and demonstrated significance in 505 of 1422 tests (p from Fisher's combined probability test = 0). We also performed the same test for the S_v of dive-sized cells within krill patches and found that only 24 of 1325 krill patches rejected the null hypothesis (Fisher's p-value = 1). This suggested that the distributions of gulps within a krill patch were often significantly different than the linearly averaged mean value in the patch. To remove any outliers due to acoustic noise

(including missing data due to dropped pings) that were missed during the data preparation process, the lowest and highest 0.5% of each day's gulp sized cells were removed from analysis.

Additional tests for acoustic artefacts

The "whale scale" level of analysis – the primary analytical scale – includes comparisons of gulp-sized cells both horizontally (across pings) and vertically (within pings). When ensonifying dense swarms, care must be taken to ensure that neither artefacts due to extinction (e.g. Foote 1990), nor artefacts in the opposite direction due to multiple scattering (Stanton 1983) influence results. In some cases these two artefacts may offset (Stanton 1983), but in both cases they are more prevalent when ensonifying organisms with stronger TS. These effects are mostly relevant when enumerating fish (with TS ~ -50 to -20 dB, Foote 1980) but have been observed to lesser extents in larger krill species like *E. superba* (TS @ 40 mm ~ -77 dB, Conti & Demer 2006), and are not commonly reported with extremely small TS of the krill in our ecosystem (~-93 dB). However, to confirm that our results are not influenced by these effects, we examined both gulp density as a function of location in the water column as well as the strength of the bottom return echo in dense krill and outside of dense krill. If gulp depth is plotted against S_{v_gulp}, no relationship is noted ($r^2 = 0.036$), and if a Generalized Linear Mixed Effects model (GLME) is run treating each column of data as a random effect, a slightly increasing relationship is noted (slope estimate 0.08 dB/gulp height, $p < 0.001$) implying that any extinction effect would be small. When examining the bottom echo, we calculated the strength of all bottom echoes for data from 05 Nov 2015, the day shown in Fig. 4, in which we recorded some of the strongest returns near the bottom that would be strong candidates to demonstrate acoustic artefacts (if they were present). Bottom return in each ping was calculated in two ways: as the sum of scattering (S_a) from 0.5 to 5.5 m below the sounder detected bottom, and as the 95th percentile of 0.1 m S_v bins in the same depth window. Comparisons of bottom strength in strongly scattering regions to adjacent regions were either not significantly different or had small differences in opposing directions (Fig S2). We also compared S_a in that 5 m bin below the bottom line to S_a in the water column above the line (down to 1.5 m above the line) in Fig S3 and found nearly no relationship. The small size of these effects, combined

with the inconsistent direction, suggests that any effect would be small and less than the error of the estimates of the means in the whale scale analysis. When applying our approach to new ecosystems with more reflective target organisms, similar precautions should be taken.

Similarly, the stochasticity inherent in acoustic data suggests that precautions should be taken to ensure that gulp-sized cells are large enough to include sufficient pings to accurately represent biomass (Foote 1983; Simmonds & MacLennan 2008). Our gulp-sized cells in Monterey averaged 9.4 ± 12.5 pings (mean ± *SD*), while in South Africa humpback whale gulp-sized cells averaged 8.4 ± 6.8 pings. To ensure cells with only a single ping were never used, in South Africa all pairs of pings were averaged into a single ping using the ping-reduction feature in Echoview. It was subsequently determined that this step made for more complicated post-processing as different ping indices were then employed for the analysis of raw and processed data. In Monterey data processing, then, an updated approach was used to simplify post-processing. All data was extracted in gulp-sized cells, but then any cell containing only a single ping was averaged into the subsequent cell (and that cell's ping number was increased by one).

Finally, it should be noted that there are many avenues for error propagation when converting acoustic backscatter to biomass: krill, which can swarm facing any direction (Calise 2009), have orientation-dependent TS (Conti & Demer 2006; Levine, Williams & Ressler 2018), efforts to ground truth estimates are inhibited by unknown krill escape from nets (Everson & Bone 1986; Brierley 1999) which may be size dependent (Hill *et al.* 1996), even with concurrent net-sampling the krill ensonified may be of different size classes than the krill sampled, krill may be oriented in different directions throughout a swarm (Hamner & Hamner 2000), and all models are subject to normal stochastic variation (Simmonds & MacLennan 2008). In any distribution, the multiplicative geomean and GSD will be more robust to some of these errors than linear summary statistics.

We report derived biomass units using the best available techniques as they are the most biologically relevant, but we also report the directly measured backscatter data in all cases so that any future improved models may be retroactively applied, including models that may directly link acoustic backscatter of krill with energy content, as proposed in Benoit-Bird and Au (2002). For comparability, all statistical

comparisons were based on log-transformed data (S_v data before biomass conversion) and were only performed within (not across) ecosystems.

Estimating overall intake

The whale scale method described herein is recommended for describing the distribution of resources within large patches or within a larger region. Calculating the distribution of biomass within cells the size of a whale's dive gives a representation of the likelihood that prey of a given biomass is encountered by a foraging whale, and reporting summary variables of lognormal distributions allows distributions in different environments to be statistically compared. However, a whale foraging in this environment will consume on average more biomass per gulp than the geomean biomass due to the right-skew of the lognormal distribution (i.e., the mean of a lognormal distribution is higher than its geomean which is equivalent to the median). If a whale samples randomly from a given dive-sized cell, the expected amount of prey consumed would be given by the number of lunges (n) multiplied by the arithmetic mean biomass of the cell (B_{dive}). B_{dive} can be estimated from the geomean and GSD parameters of the lognormal distribution of biomass in gulp-sized cells (B_{gulp}). If we define parameters μ = log(geomean(B_{gulp})) and σ = log(GSD(B_{gulp})) to be the mean and standard deviation of log(B_{gulp}) in a dive-sized cell, then the estimated mean biomass density engulfed by a randomly lunging whale (denoted $\widehat{B_{dive}}$ to signify that it is a calculated parameter derived from the distribution) can be calculated from these parameters using any of these equivalent formulas for the expectation of the lognormal distribution:

$$\widehat{B_{dive}} = e^{\mu+\sigma^2/2} = e^{\mu\cdot\log(b)+(\sigma\cdot\log(b))^2/2} = e^{\log(\text{geomean})+(\log(\text{GSD}))^2/2} \qquad \text{(eq. 2)}$$

where b is the base of the logarithm used to calculate μ and σ and "log" is the natural logarithm. If we wish to estimate the linearized mean of acoustic backscatter from mean(S_{v_gulp}) and SD(S_{v_gulp}), i.e., the parameters of ${}_N S_{v\_ws}$, directly without first back transforming to linear units, it can be derived from eq. 2 that:

$$\widehat{S_{v\_dive}} = \text{mean}(S_{v_{gulp}}) + \left(SD(S_{v_{gulp}})\right)^2 \cdot \frac{\log(10)}{20} \qquad \text{(eq. 3)}$$

Calculating $\hat{B}$ directly using eq. 2 or indirectly using the results of eq. 3 would be equivalent to directly calculating the mean biomass if biomass data were perfectly lognormally distributed. In natural environments, calculating $\hat{B}$ from distribution parameters may be more robust than calculating mean biomass directly since lognormal parameters are more robust to outliers and acoustic artefacts. Summarizing data at spatial scales relevant to predators is also more likely to reflect the mean prey encountered by predators (Haeckel 1893; Stephens & Krebs 1986) than, for instance, averaging patches of different sizes or looking at the mean of all patches combined. Thus, the biomass expected to be consumed from a randomly foraging predator could be calculated from eq. 2 using the geomean and GSD of all $\widehat{B_{dive}}$ (or, equivalently, the mean and *SD* of $\widehat{S_{v\_dive}}$) in a region. Because predators are likely to forage with some degree of discrimination about what part of a patch they forage in, we suggest that biomass calculated as described above would be a lower bound for an estimate of consumption, while employing the same procedure using parameters at the informed whale scale (using only the densest half of gulp-sized cells within dive-sized cells) could be a more accurate estimate.

Figures & Tables

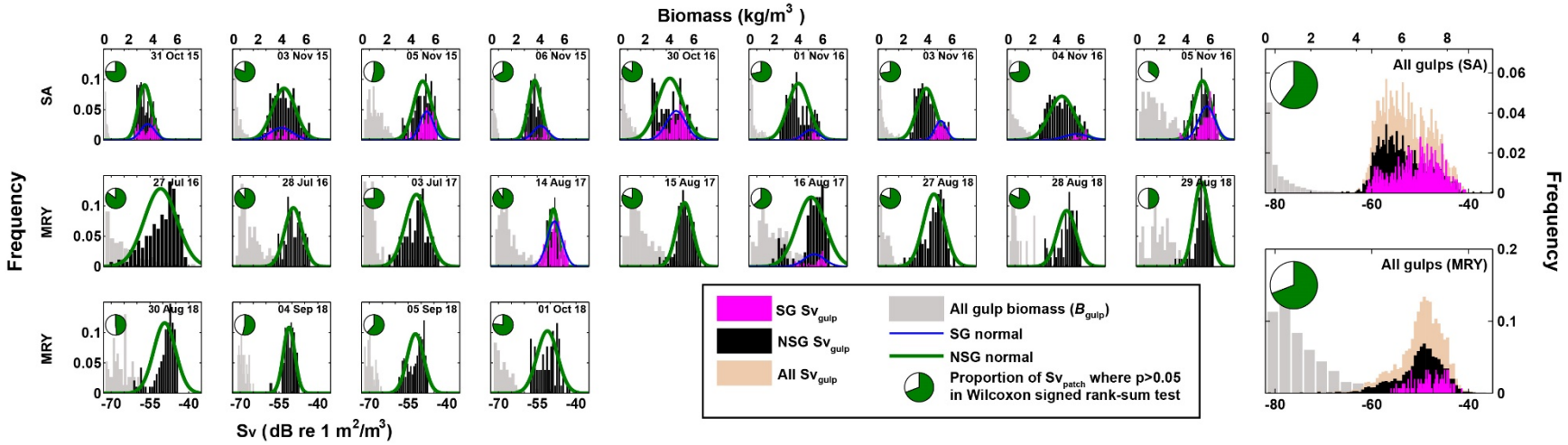

Fig. S1- Distribution of gulp sized cells of acoustic energy (tan, black and magenta) bars and biomass (grey bars) for each day. Acoustic energy (described in logarithmic units) is approximately normally distributed while biomass is skewed. Green pie charts show the proportion of identified krill patches that day for which the null hypothesis, that the distribution of Sv_{gulp} within the patch is centered around Sv_{patch}, could not be rejected at the $p < 0.05$ significance level according to the Wilcoxon signed rank-sum test.

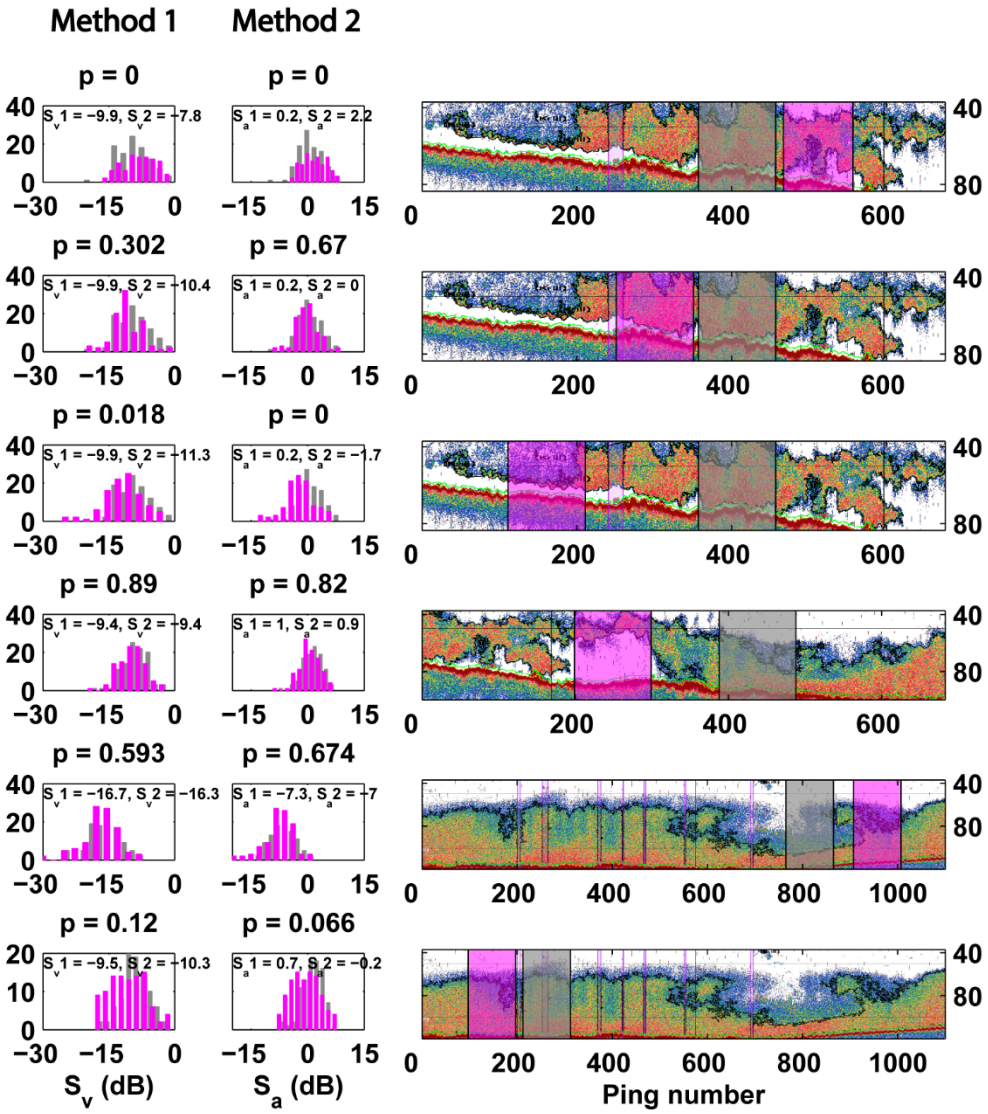

Fig. S2- Comparisons of bottom echo strength in adjacent regions of varying water column echos, for determining if there is an acoustic shadowing effect from dense scatterers. Gray regions have higher water column strength and pink regions have lower water column strength, histograms are plots of all pings in the highlighed regions. Method 1- the 95th percentile of 0.1 m S_v bins 0.5 to 5.5 m below the sounder-detected bottom for each ping. Method 2- the sum of scattering (S_a) from 0.5 to 5.5 m below the sounder-detected bottom. Data was collected at 200 kHz data on 05 Nov 2015.

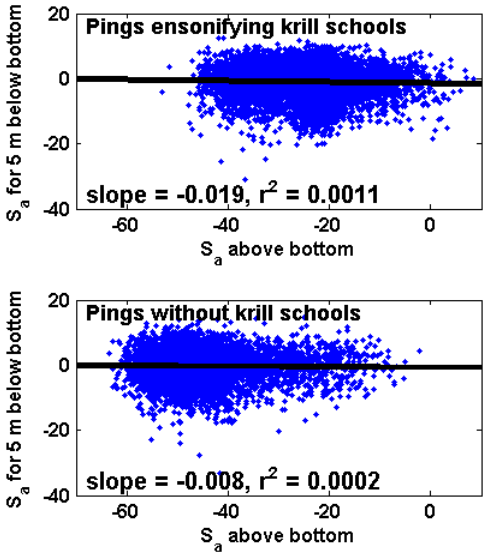

Fig. S3- Plots of S_a for each 200 kHz ping on 05 Nov 2015 from 0.5 to 5.5 m below the sounder-detected bottom as a function of S_a in the water column. The flat lines suggests no (or very minimal) acoustic shadowing effects.

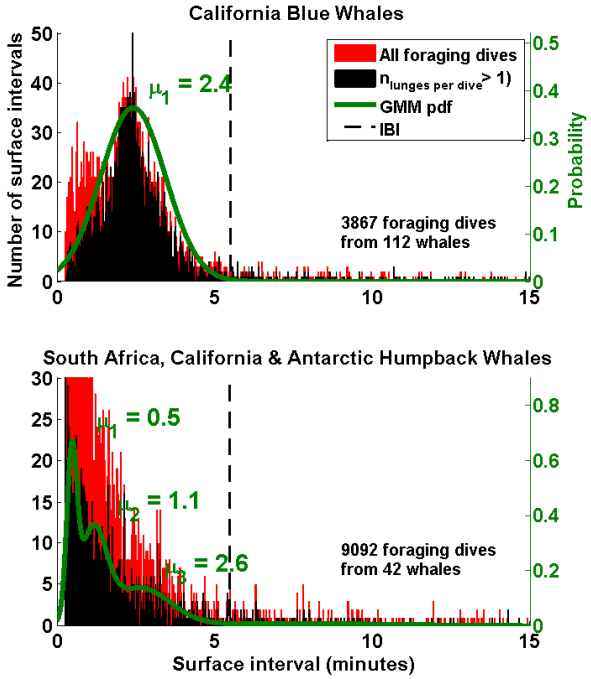

Fig. S4- Surface interval between foraging dives for blue whales and humpback whales tagged in multiple ecosystems. Black bars are surface intervals from foraging dives with at least 2 lunges until the next foraging dive. Red is the surface intervals for all foraging dives. For both species, the surface interval duration corresponding to the mean of the largest fitted Gaussian curve in the bulk of the data + 3 *SD* was used to differentiate "foraging bouts." That is, a "foraging bout" was defined as the combined duration of all dives where the surface interval between dives with foraging effort was less than 5.5 minutes (the dashed vertical bar in both plots). The duration of a foraging bout was defined from the start of the first dive to 5.5 minutes after the last foraging dive.

Table S1- Summary of data collected near super-groups (SG)

Region	*Date*	*Hrs prey mapping near SG*	*Hrs prey mapping near feeding whales not in SG*	*Estimated SG size (best estimate number of animals)*	*Time prey data collection around SG began*	*Number of tagged whales in SG (total hrs)*
South Africa (*M. novaeangliae*)	31-Oct-2015	1.3	3.5	50	13:08	2 (4.5)
	3-Nov-2015	0.6	10.2	—	20:42	1 (3.7)
	5-Nov-2015	0.8	1.1	150	17:41	0 (—)
	6-Nov-2015	0.9	3.8	25	8:04	0 (—)
	30-Oct-2016	0.9	7.6	45	18:32	0 (—)
	1-Nov-2016	0.7	2.5	60	8:34	0 (—)
	3-Nov-2016	3.9	4.2	80	7:33	0 (—)
	4-Nov-2016	0.9	6.3	60	9:53	0 (—)
	5-Nov-2016	2.0	2.8	50	7:07	1 (0.9)
	6-Nov-2016	—	—	50	—	1 (5.7)
	7-Nov-2016	—	—	75	—	1 (1.7)
Monterey (*B. musculus*)	14-Aug-2017	0.9	1.8	25	10:19	2 (5.0)
	16-Aug-2017	0.8	5.0	15	13:32	4 (5.5)
	Combined other days	—	32.3	—	—	—

Table S2- Feeding parameters from tag data for individual whales while they were foraging in super-groups compared to when then were not within a super-group. Each row is a unique tag ID of the format spYYMMDD-tag#, where sp = species ID (mn for humpback whales, bw for blue whales), year, month, day and tag number.

M. novaeangliae **(South Africa)**	*Feeding rate (lunges per hr within a feeding bout)*		*Inter lunge interval (ILI, s)*		*Inter lunge search area (10^2 m^2)*		*Lunges per dive*	
Tag ID	SG	NSG	SG	NSG	SG	NSG	SG	NSG
mn151031-3	58.3	—	34 ± 8	—	3.1 ± 1.3	—	6.7 ± 2.1	—
mn151031-4	62.7	63.8	30 ± 9	35 ± 9	3.9 ± 2.6	4.7 ± 4.4	6.2 ± 1.4	2.9 ± 1.0
mn151103-7	77.3	45.1	33 ± 11	39 ± 20	3.3 ± 3.2	9.2 ± 14.5	3.7 ± 1.9	7.6 ± 3.5
mn161105-36	37.5	20.5	32 ± 9	33 ± 34	4.0 ± 3.0	—	3.8 ± 0.9	2.5 ± 0.7
mn161106-36b	55.9	21.3	32 ± 10	70 ± 30	4.0 ± 2.4	11 ± 9.3	3.5 ± 1.3	2.9 ± 0.8
mn161107-36b	38.5	35.3	31 ± 10	21 ± 3	2.3 ± 0.8	—	2.9 ± 1.0	2.2 ± 0.4
B. musculus **(Monterey Bay)**								
Tag ID	SG	NSG	SG	NSG	SG	NSG	SG	NSG
bw170814-40	23.8	27.0	94 ± 13	93 ± 19	27 ± 14	39 ± 31	4.6 ± 1.1	3.5 ± 1.3
bw170814-50	22.6	19.4	96 ± 19	102 ± 17	51 ± 39	54 ± 27	4.0 ± 0.9	3.1 ± 0.9
bw170816-23	29.2	—	81 ± 8	—	33 ± 12	—	4.2 ± 0.4	—
bw170816-42	21.1	14.2	103 ± 23	104 ± 6	40 ± 46	38 ± 6.3	3.1 ± 1.0	2.8 ± 1.3
bw170816-44	26.1	24.8	89 ± 17	101 ± 21	49 ± 46	51 ± 65	3.9 ± 0.6	3.4 ± 1.6
bw170816-51	22.6	18.4	107 ± 5	111 ± 13	17 ± 1.6	29 ± 16	4.0 ± 0.6	3.9 ± 1.2

Table S3- Prey in super group (SG) regions and in regions where whales are present but not aggregated (NSG). SA = South Africa, MRY = Monterey.

Panel A: Humpback whales

	Patch biomass ($_{LN}B_{patch}$) *in kg m^{-3}* ($_{N}S_{v\ patch}$ *in dB*)			*Whale scale biomass* ($\overline{_{LN}B_{ws}}$) *in kg m^{-3}* ($_{N}S_{v\ ws}$ *in dB*)			*Informed whale scale* (*informed* $\overline{_{LN}B_{ws}}$) *in kg m^{-3}* (*informed* $_{N}S_{v\ ws}$ *in dB*)			*Patch thickness (m)*			*Whale scale SD (dB)*			*Informed whale scale SD (dB)*		
Date of SG	SG		NSG	SG		NSG	SG		NSG	SG		NSG	SG		NSG	SG		NSG
31-Oct-2015	0.12 ·: 1.8 (-56.8 ± 2.4)	*	0.09 ·: 1.7 (-58.1 ± 2.2)	0.17 ·: 1.7 (-55.2 ± 2.3)	***	0.14 ·: 1.8 (-56.3 ± 2.4)	0.27 ·: 1.3 (-53.2 ± 1.2)	**	0.24 ·: 1.4 (-53.8 ± 1.5)	23 ± 12	***	10 ± 8	2.3		2.4	1.2	***	1.5
3-Nov-2015	*0.19 ·: 2.5 (-54.7 ± 4.1)*		*0.29 ·: 2.8 (-53.0 ± 4.4)*	*0.27 ·: 2.2 (-53.3 ± 3.3)*		*0.32 ·: 2.1 (-52.6 ± 3.3)*	0.66 ·: 1.5 (-49.4 ± 1.6)	*	0.51 ·: 1.6 (-50.6 ± 2.0)	21 ± 15	***	3 ± 3	*3.3*		*3.3*	1.6	***	2.0
5-Nov-2015	*0.33 ·: 4.3 (-52.4 ± 6.3)*		*0.34 ·: 2.2 (-52.3 ± 3.5)*	0.84 ·: 1.9 (-48.3 ± 2.8)	*	0.61 ·: 2.2 (-49.7 ± 3.4)	1.39 ·: 1.3 (-46.2 ± 1.3)	*	1.15 ·: 1.5 (-47.0 ± 1.6)	37 ± 10	***	23 ± 13	2.8		3.4	1.3	***	1.6
6-Nov-2015	0.22 ·: 2.2 (-54.1 ± 3.5)		0.13 ·: 1.7 (-56.5 ± 2.4)	0.27 ·: 2.0 (-53.3 ± 3.0)	***	0.15 ·: 1.9 (-55.7 ± 2.7)	0.47 ·: 1.4 (-50.9 ± 1.3)	***	0.27 ·: 1.4 (-53.3 ± 1.5)	30 ± 19	***	8 ± 7	*3.0*		*2.7*	1.3	***	1.5
30-Oct-2016	0.45 ·: 2.1 (-51.1 ± 3.3)	**	0.21 ·: 3.3 (-54.4 ± 5.2)	0.46 ·: 2.4 (-50.1 ± 3.8)		0.28 ·: 2.2 (-53.1 ± 3.5)	1.07 ·: 1.5 (-47.3 ± 1.8)		—	8 ± 5	***	3 ± 2	*3.8*		*3.5*	1.8		—
1-Nov-2016	0.84 ·: 1.6 (-48.4 ± 2.1)	***	0.17 ·: 2.2 (-55.2 ± 3.4)	0.59 ·: 2.1 (-49.9 ± 3.3)	*	0.35 ·: 2.8 (-52.2 ± 4.4)	*1.34 ·: 1.4 (-46.3 ± 1.4)*		*1.46 ·: 1.6 (-46.0 ± 2.0)*	15 ± 7	***	6 ± 5	3.3		4.4	1.4	***	2.0
3-Nov-2016	0.75 ·: 1.8 (-48.8 ± 2.7)	***	0.15 ·: 2.0 (-55.8 ± 3.0)	0.70 ·: 1.9 (-49.2 ± 2.8)	***	0.29 ·: 2.1 (-53.0 ± 3.3)	1.14 ·: 1.3 (-47.0 ± 1.1)	***	0.63 ·: 1.4 (-49.6 ± 1.5)	34 ± 7	***	8 ± 7	2.8		3.3	1.1	***	1.5
4-Nov-2016	1.56 ·: 3.3 (-45.7 ± 5.2)	**	0.25 ·: 2.7 (-53.7 ± 4.3)	1.23 ·: 2.3 (-46.7 ± 3.6)	***	0.51 ·: 2.3 (-50.5 ± 3.6)	2.31 ·: 1.4 (-44.0 ± 1.4)	***	1.28 ·: 1.5 (-46.5 ± 1.6)	23 ± 8	***	7 ± 8	3.6		3.6	1.4	***	1.6
5-Nov-2016	1.22 ·: 2.3 (-46.7 ± 3.6)		1.05 ·: 2.9 (-47.4 ± 4.7)	1.11 ·: 2.3 (-47.1 ± 3.5)	*	0.82 ·: 2.4 (-48.4 ± 3.8)	2.15 ·: 1.4 (-44.3 ± 1.4)	**	1.75 ·: 1.4 (-45.2 ± 1.6)	19 ± 8	***	14 ± 7	3.5		3.8	1.4	***	1.6
All SA	0.35 ·: 3.4 (-52.1 ± 5.3)	***	0.18 ·: 2.6 (-55.1 ± 4.2)	0.49 ·: 2.0 (-50.7 ± 3.0)	***	0.31 ·: 2.1 (-52.7 ± 3.3)	0.91 ·: 1.3 (-48.0 ± 1.3)	***	0.66 ·: 1.4 (-49.4 ± 1.6)	22 ± 14	***	8 ± 9	3.0	**	3.3	1.3	***	1.6

Panel B: Blue whales

Date of SG	SG		NSG	SG		NSG	SG		NSG	SG		NSG	SG		NSG	SG		NSG
14-Aug-2017	*0.84 ·: 2.0 (-50.0 ± 3.0)*		*1.09 ·: 1.8 (-48.9 ± 2.5)*	1.38 ·: 1.6 (-47.8 ± 2.0)	*	1.07 ·: 1.7 (-48.9 ± 2.2)	1.95 ·: 1.3 (-46.3 ± 1.0)	***	1.41 ·: 1.3 (-47.7 ± 1.3)	24 ± 24	***	14 ± 14	2.0		2.2	1.0	***	1.3
16-Aug-2017	0.95 ·: 2.8 (-49.4 ± 4.5)		0.70 ·: 4.5 (-50.8 ± 6.5)	1.74 ·: 1.7 (-46.8 ± 2.4)		1.54 ·: 1.8 (-47.3 ± 2.5)	2.74 ·: 1.3 (-44.8 ± 1.0)	***	2.35 ·: 1.3 (-45.5 ± 1.1)	50 ± 24	***	20 ± 15	2.4		2.5	1.0	***	1.1
All MRY	0.87 ·: 2.1 (-49.8 ± 3.3)	*	0.67 ·: 3.7 (-50.9 ± 5.7)	1.49 ·: 1.6 (-47.5 ± 2.2)	***	1.19 ·: 1.8 (-48.5 ± 2.6)	2.22 ·: 1.3 (-45.8 ± 1.0)	***	1.89 ·: 1.3 (-46.5 ± 1.2)	33 ± 27	***	15 ± 15	2.2	**	2.6	1.0	***	1.2

Comparisons (* = p<0.05, ** = p<0.01, *** = p<0.001). *Italics* indicates an effect in the opposite direction of the prevalance of data

— = data collected on this day did not meet the threshold of at least 30 gulps per dive

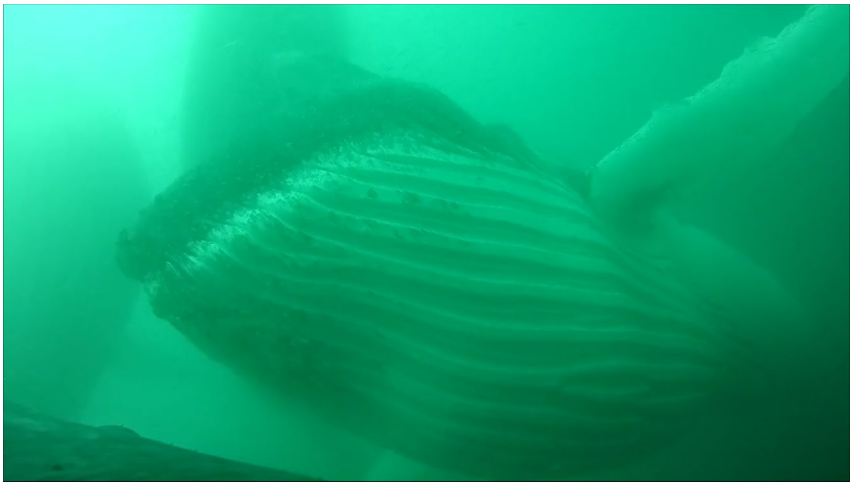

Video S1- On animal video from humpback whales foraging within super-groups. High quality version available with deposited data at: https://purl.stanford.edu/rq794kc6747

References

Atkinson, A., Siegel, V., Pakhomov, E., Jessopp, M. & Loeb, V. (2009) A re-appraisal of the total biomass and annual production of Antarctic krill. *Deep Sea Research Part I: Oceanographic Research Papers,* **56,** 727-740.

Barange, M. (1994) Acoustic identification, classification and structure of biological patchiness on the edge of the Agulhas Bank and its relation to frontal features. *South African Journal of marine science,* **14,** 333-347.

Benoit-Bird, K.J. & Au, W.W.L. (2002) Energy: Converting from acoustic to biological resource units. *The Journal of the Acoustical Society of America,* **111,** 2070-2075.

Brierley, A.S. (1999) A comparison of Antarctic euphausiids sampled by net and from geothermally heated waters: insights into sampling bias. *Polar Biology,* **22,** 109-114.

Cade, D.E., Barr, K.R., Calambokidis, J., Friedlaender, A.S. & Goldbogen, J.A. (2018) Determining forward speed from accelerometer jiggle in aquatic environments. *Journal of Experimental Biology,* **221,** jeb170449.

Cade, D.E. & Benoit-Bird, K.J. (2014) An automatic and quantitative approach to the detection and tracking of acoustic scattering layers. *Limnology and Oceanography: Methods,* **12,** 742-756.

Cade, D.E., Friedlaender, A.S., Calambokidis, J. & Goldbogen, J.A. (2016) Kinematic Diversity in Rorqual Whale Feeding Mechanisms. *Current Biology,* **26,** 2617-2624.

Calise, L. (2009) Multifrequency acoustic target strength of northern krill.

CCAMLR (2005) Report of the twenty fourth meeting of the Scientific Committee. SC-CAMLR-XXIV. *Commission for the Conservation of Antarctic Marine Living Resources.* *https://www.ccamlr.org/en/system/files/e-sc-xxix-a5.pdf*. Hobart, Australia.

Coetzee, J. (2000) Use of a shoal analysis and patch estimation system (SHAPES) to characterise sardine schools. *Aquatic Living Resources,* **13,** 1-10.

Conti, S.G. & Demer, D.A. (2006) Improved parameterization of the SDWBA for estimating krill target strength. *ICES Journal of Marine Science: Journal du Conseil,* **63,** 928-935.

Croll, D.A., Marinovic, B., Benson, S., Chavez, F.P., Black, N., Ternullo, R. & Tershy, B.R. (2005) From wind to whales: trophic links in a coastal upwelling system. *Marine Ecology Progress Series,* **289,** 117-130.

Croll, D.A., Newton, K.M., Marinovic, B.B. & Ralston, S. (2009) Critical Prey Species in the Monterey Bay National Marine Sanctuary. pp. 38. UC Santa Cruz.

De Robertis, A. & Higginbottom, I. (2007) A post-processing technique to estimate the signal-to-noise ratio and remove echosounder background noise. *ICES Journal of Marine Science,* **64,** 1282-1291.

Demer, D., Berger, L., Bernasconi, M., Bethke, E., Boswell, K., Chu, D. & Domokos, R. (2015) Calibration of acoustic instruments. *ICES Cooperative Research Report,* **326,** 133.

Demer, D.A. & Martin, L.V. (1995) Zooplankton target strength: Volumetric or areal dependence? *The Journal of the Acoustical Society of America,* **98,** 1111-1118.

Everson, I. & Bone, D. (1986) Effectiveness of the RMT8 system for sampling krill (*Euphausia superba*) swarms. *Polar Biology,* **6,** 83-90.

Findlay, K.P., Seakamela, S.M., Meÿer, M.A., Kirkman, S.P., Barendse, J., Cade, D.E., Hurwitz, D., Kennedy, A., Kotze, P.G.H., McCue, S.A., Thornton, M., Vargas-Fonseca, O.A. & Wilke, C.G. (2017) Humpback whale "super-groups" – A novel low-latitude feeding behaviour of Southern Hemisphere humpback whales (*Megaptera novaeangliae*) in the Benguela Upwelling System. *PLoS ONE,* **12,** e0172002.

Foote, K.G. (1980) Averaging of fish target strength functions. *The Journal of the Acoustical Society of America,* **67,** 504-515.

Foote, K.G. (1983) Linearity of fisheries acoustics, with addition theorems. *The Journal of the Acoustical Society of America,* **73,** 1932-1940.

Foote, K.G. (1990) Correcting acoustic measurements of scatterer density for extinction. *The Journal of the Acoustical Society of America,* **88,** 1543-1546.

Ghasemi, A. & Zahediasl, S. (2012) Normality tests for statistical analysis: a guide for non-statisticians. *International journal of endocrinology and metabolism,* **10,** 486.

Goldbogen, J.A., Cade, D.E., Wisniewska, D.M., Potvin, J., Segre, P.S., Savoca, M.S., Hazen, E.L., Czapanskiy, M.F., Kahane-Rapport, S.R., DeRuiter, S.L., Gero, S., Tønnesen, P., Gough, W.T., Hanson, M.B., Holt, M., Jensen, F.H., Simon, M., Stimpert, A.K., Arranz, P., Johnston, D.W., Nowacek, D.P., Parks, S.E., Visser, F., Friedlaender, A.S., Tyack, P.L., Madsen, P.T. & Pyenson, N.D. (2019) Why whales are big but not bigger: Physiological drivers and ecological limits in the age of ocean giants. *Science,* **366,** 1367-1372.

Goldbogen, J.A., Calambokidis, J., Shadwick, R.E., Oleson, E.M., McDonald, M.A. & Hildebrand, J.A. (2006) Kinematics of foraging dives and lunge-feeding in fin whales. *Journal of Experimental Biology,* **209,** 1231-1244.

Haeckel, E. (1893) Planktonic studies: a comparative investigation of the importance and constitution of the pelagic fauna and flora. *Report of the US Commissioner of Fish and Fisheries for 1889 to 1893***,** 565-641.

Hamner, W.M. & Hamner, P.P. (2000) Behavior of Antarctic krill (Euphausia superba): schooling, foraging, and antipredatory behavior. *Canadian Journal of Fisheries and Aquatic Sciences,* **57,** 192-202.

Hazen, E.L., Friedlaender, A.S. & Goldbogen, J.A. (2015) Blue whale (*Balaenoptera musculus*) optimize foraging efficiency by balancing oxygen use and energy gain as a function of prey density. *Science Advances,* **1,** e1500469.

Hill, H., Trathan, P., Croxall, J. & Watkins, J. (1996) A comparison of Antarctic krill Euphausia superba caught by nets and taken by macaroni penguins Eudyptes chrysolophus: evidence for selection? *Marine Ecology Progress Series,* **140,** 1-11.

Jarvis, T., Kelly, N., Kawaguchi, S., van Wijk, E. & Nicol, S. (2010) Acoustic characterisation of the broad-scale distribution and abundance of Antarctic krill (*Euphausia superba*) off East Antarctica (30-80 E) in January-March 2006. *Deep Sea Research Part II: Topical Studies in Oceanography,* **57,** 916-933.

Johnson, M.P. & Tyack, P.L. (2003) A digital acoustic recording tag for measuring the response of wild marine mammals to sound. *IEEE Journal of Oceanic Engineering,* **28,** 3-12.

Levine, M., Williams, K. & Ressler, P.H. (2018) Measuring the in situ tilt orientation of fish and zooplankton using stereo photogrammetric methods. *Limnology and Oceanography: Methods,* **16,** 390-399.

MacLennan, D.N., Fernandes, P.G. & Dalen, J. (2002) A consistent approach to definitions and symbols in fisheries acoustics. *ICES Journal of Marine Science,* **59,** 365-369.

Mauchline, J. (1967) Volume and weight characteristics of species of Euphausiacea. *Crustaceana***,** 241-248.

MBNMS (2009) Monterey Bay National Marine Sanctuary Condition Report 2009.

McGarry, L. (2014) An Examination Of Blue Whale Foraging And Its Krill Prey Field In The Monterey Bay Submarine Canyon.

Nickels, C.F., Sala, L.M. & Ohman, M.D. (2018) The morphology of euphausiid mandibles used to assess selective predation by blue whales in the southern sector of the California Current System. *Journal of Crustacean Biology,* **38,** 563-573.

Nickels, C.F., Sala, L.M. & Ohman, M.D. (2019) The euphausiid prey field for blue whales around a steep bathymetric feature in the southern California current system. *Limnology and Oceanography,* **64,** 390-405.

Pérez Seijas, G.M. (1987) Relaciones de talla, peso y volumen en *Euphausia vallentini*, *E. Lucens* y *Thysanoessa gregaria* (Euphausiacea, Eucarida).[*Euphausia vallentini, E. Lucens* and *Thysanoessa gregaria* (Euphausiacea, Eucarida) length, volume and weight relationships]. *Physis A,* **45,** 61-68.

Ryan, T.E., Downie, R.A., Kloser, R.J. & Keith, G. (2015) Reducing bias due to noise and attenuation in open-ocean echo integration data. *ICES Journal of Marine Science,* **72,** 2482-2493.

Santora, J.A., Ralston, S. & Sydeman, W.J. (2011) Spatial organization of krill and seabirds in the central California Current. *ICES Journal of Marine Science,* **68,** 1391-1402.

Schoenherr, J.R. (1991) Blue whales feeding on high concentrations of euphausiids around Monterey Submarine Canyon. *Canadian Journal of Zoology,* **69,** 583-594.

Simmonds, J. & MacLennan, D.N. (2008) *Fisheries acoustics: theory and practice*. John Wiley & Sons.

Simon, M., Johnson, M. & Madsen, P.T. (2012) Keeping momentum with a mouthful of water: behavior and kinematics of humpback whale lunge feeding. *The Journal of Experimental Biology,* **215,** 3786-3798.

Southall, B.L., DeRuiter, S.L., Friedlaender, A., Stimpert, A.K., Goldbogen, J.A., Hazen, E., Casey, C., Fregosi, S., Cade, D.E. & Allen, A.N. (2019) Behavioral responses of individual blue whales (*Balaenoptera musculus*) to mid-frequency military sonar. *Journal of Experimental Biology,* **222,** jeb190637.

Stanton, T.K. (1983) Multiple scattering with applications to fish-echo processing. *The Journal of the Acoustical Society of America,* **73,** 1164-1169.

Stanton, T.K. & Chu, D. (2000) Review and recommendations for the modelling of acoustic scattering by fluid-like elongated zooplankton: euphausiids and copepods. *ICES Journal of Marine Science,* **57,** 793-807.

Stanton, T.K., Chu, D. & Wiebe, P.H. (1998) Sound scattering by several zooplankton groups. II. Scattering models. *The Journal of the Acoustical Society of America,* **103,** 236.

Stanton, T.K., Wiebe, P.H., Chu, D., Benfield, M.C., Scanlon, L., Martin, L. & Eastwood, R.L. (1994) On acoustic estimates of zooplankton biomass. *ICES Journal of Marine Science: Journal du Conseil,* **51,** 505-512.

Stephens, D.W. & Krebs, J.R. (1986) *Foraging theory*. Princeton University Press.

Warren, J.D., Stanton, T.K., Benfield, M.C., Wiebe, P.H., Chu, D. & Sutor, M. (2001) In situ measurements of acoustic target strengths of gas-bearing siphonophores. *ICES Journal of Marine Science,* **58,** 740-749.

Wilson, R.P., Liebsch, N., Davies, I.M., Quintana, F., Weimerskirch, H., Storch, S., Lucke, K., Siebert, U., Zankl, S. & Müller, G. (2007) All at sea with animal tracks; methodological and analytical solutions for the resolution of movement. *Deep Sea Research Part II: Topical Studies in Oceanography,* **54,** 193-210.